Compare the physicochemical properties of engineered polymer-functionalized silver nanoparticles and evaluate their biological properties against *Porphyromonas gingivalis*

meng zhang (zmeng@hku.hk)
University of Hong Kong - Kennedy Town Center https://orcid.org/0000-0002-2069-9862
Edward CM. Lo
University of Hong Kong - Kennedy Town Center https://orcid.org/0000-0002-3618-0619

Research Article

Keywords: Silver nanoparticles, polymers, Porphyromonas gingivalis, antibacterial, antibiofilm, cytotoxicity

Posted Date: March 7th, 2022

DOI: https://doi.org/10.21203/rs.3.rs-1410184/v1

Abstract

Background: Nano silver (AgNPs) is a broad-spectrum antibacterial nanomaterial and many polymer-functionalized AgNPs (P-AgNPs) have been developed to optimize the biological properties of AgNPs and some possess good potential for commercial application. However, no horizontal study compares the differences in physicochemical and biological properties among various P-AgNPs, and provides evidence for the selection of polymer and optimization of AgNPs.

Methods: Two AgNPs with similar nano-size but opposite surface charges were synthesized and functionalized by seven polymers. Their physicochemical properties were detected by UV-Vis, DLS, TEM and ICP-OES. Their biological properties against *Porphyromonas gingivalis* and human gingival fibroblast were investigated by MIC determination, time-dependent antibacterial assay, antibiofilm activity, and cell viability assay. Silver diamine fluoride (SDF), $AgNO_3$ and metronidazole were used as the positive controls.

Results: Comparative analysis found that there was no significant difference between P-AgNPs and AgNPs in nano-size and surface charge. For antibacterial property, in negatively charged AgNPs, only polyvinylpyrrolidone (PVP)-functionalized AgNPs-1 showed significant lower MIC values than AgNPs-1 (0.79 vs 4.72 μg/ml). In positively charged AgNPs, the MIC values of all P-AgNPs (0.34-4.37 μg/ml) were lower than AgNPs-2 (13.89 μg/ml), especially the PVP- and Pluronic127-AgNPs-2 (1.75 and 0.34 μg/ml). For antibiofilm property, the PVP-AgNPs-1 (7.86 μg/ml, P=0.002) and all P-AgNPs-2 (3.425-31.14 μg/ml, P<0.001) showed great antibiofilm effect against *Porphyromonas gingivalis* biofilm at 5* to 10* MIC level. For cytotoxicity, all negatively charged AgNPs and PVP-AgNPs-2 showed no cytotoxicity at MIC level, but significant cytotoxicity was detected at 2.5*-10* MIC levels.

Conclusions: Polymer functionalization only minimally alters the physical properties of AgNPs, but modifies their surface chemical property, which is closely related to their biological property. The antibacterial and antibiofilm properties and cytotoxicity of AgNPs can be significantly optimized to varying degrees by some polymer functionalization, especially using PVP. However, none of the AgNPs studied has low cytotoxicity at the antibiofilm concentration levels.

Background

Silver ion is an effective metal antibacterial element with a long history of application [1]. With the advance of nanoscience and nanotechnology, silver nanoparticles (AgNPs) are developed to provide a wider variety of physical, chemical and biological properties of silver [2]. The increased antibacterial efficacy and bioavailability of AgNPs has been confirmed by research [3, 4]. AgNPs are powerful nano-weapons against bacteria, including multidrug-resistant bacteria, and possess broad application potential [5]. Some AgNPs products have been applied in biomedical field [6].

However, the safety issue caused by the exposure and accumulation of silver in the environment and in the human body cannot be ignored and has received increasing attention. Evidence from many studies

reveals that AgNPs have different interaction modes with living cells and different antibacterial mechanisms compared with silver ions, due to the large surface area and intrinsic physicochemical properties of nanomaterials [7]. However, the toxicity mechanism of AgNPs in cytoplasm is still primarily correlated with the release of silver ions [8]. Hence, in order to reduce the accumulation and toxicity of silver, many studies have been devoted to decrease the working concentration of silver by optimizing AgNPs' biological properties [9].

The biological properties of AgNPs are closely associated with their surface physicochemical properties, including nano dimension, shape, surface charge, colloidal state and surface chemical [10, 11]. Polymer functionalization is an effective way to modify the surface physicochemical properties of AgNPs and optimize their biological properties [12, 13]. Polyethylene glycol (PEG, H–(O – CH_2 – CH_2)n – OH), Polyvinylpyrrolidone (PVP) and Pluronic are representative and frequently used polymers in researches [14–16]. Both PEG and PVP are considered biologically safe, are water-soluble polymer, and have been applied in various fields, including biomedical, industry and personal care. Some PEG/PVP coated AgNPs demonstrate stronger antibacterial and antibiofilm activity [17, 18], while some show lower cytotoxicity instead of better antibacterial activity [19, 20]. In addition, Pluronic™ is a series of amphiphilic, non-ionic poly (ethylene oxide, PEO)-poly (propylene oxide, PPO)-PEO triblock copolymers with various molecular weights. They have excellent surfactant properties in dispersion, stabilization and emulsification aspects, and good biocompatibility [21], and have been used in pharmaceutical formulations [22]. Some researchers have used Pluronic to modify AgNPs, resulting in enhanced stability, and antibacterial and antibiofilm effectiveness [23, 24]. So far, no horizonal study comparing the effectiveness of different polymer-functionalization on improving the physicochemical and biological properties of AgNPs can be found. Thus, the important information on which polymer would be a better choice for optimizing the biological properties of AgNPs is lacking.

In dentistry, *Porphyromonas gingivalis* (*P. gingivalis*) is a crucial pathogen of periodontitis, and it is also associated with some systemic diseases, such as type 2 diabetes, cardiovascular disease, Alzheimer disease and aspiration pneumonia [25–28]. Inhibition of *P. gingivilis* is important for reducing the risk of periodontitis and probably also the above-mentioned systemic diseases. Therefore, *P. gingivilis* was used in the current study to compare the effect of different polymer-functionalization on the physicochemical and biological properties of AgNPs. In this study, we synthesized two AgNPs of similar nano dimensions but opposite surface charges, and then functionalized them using seven polymers with different molecular weights (PEG, PVP and Pluronic™). This study aimed to compare the physicochemical and biological properties of the engineered polymer-functionalization AgNPs, and to identify a polymer that can greatly optimize the biological property of AgNPs against *P. gingivilis*.

Methods

Synthesis of nano silver

Silver nanoparticles (AgNPs) with similar nano size but opposite surface charges were synthesized based on previously reported methods.

Negative charged AgNPs: based on Vladimir's method with slight modification [29], the following freshly prepared solutions were mix together in the following order: 7 ml of 12.5 mM TSC, 17.5 ml of 0.375 mM $AgNO_3$, 17.5 ml of 10 mM hydrogen peroxide (H_2O_2), 228 ul of 10 mM potassium bromide (KBr). Then 8 ml of 5 mM $NaBH_4$ was added dropwise into the above solution until there was no further visible color change. This brown-red product solution was the AgNPs (named AgNPs-1).

Positively charged AgNPs: based on Abbaszadegan's method with slight modification [30], 1 ml of 10 mM $AgNO_3$ was dropped into 20 ml of 6.2 mM 1-dodecyl-3-methylimidazolium chloride ([C12 mim][Cl]) aqueous solution and vigorously stirred. Then 100 ul of freshly prepared 0.4 M $NaBH_4$ was dropped into the resultant solution to obtain a golden solution of AgNPs (named AgNPs-2).

Synthesis of polymer-functionalized AgNPs (P-AgNPs)

PEG, PVP, and Pluronic™ with different weight molecular, including PEG 400, PEG 2000, PEG-SH 5000, PVP (MW 10000), Pluronic P103 (Mn 5000), P123 (Mn 5800), and F127 (Mn 12000), were used to functionalized the synthesized AgNPs. The molar ratio of Ag ion and polymer PEG/PVP was set as 1:4, and the polymers were freshly pre-dissolved in 10 ml of sterile DI water. The Pluronic™ products were directly added to the AgNPs solutions at the value lower than the CMC (critical micelle concentration) value, the CMC value of P103, P123, and F127 were 0.1 mg/ml, 0.052 mg/ml and 1 mg/ml, respectively. Polymer solution/powder of appropriate concentration and weight was added to the corresponding synthetic AgNPs solution to encapsulate the AgNPs, and then the product solutions were stirred overnight for full reaction.

All AgNPs solutions were centrifuged and washed three times at 15000 rpm for 15 min each to remove the excess unreacted ionic liquid. The pellet was then resuspended in 200 ul of sterile DI water and the AgNPs-1/2 and P-AgNPs-1/2 products were stored at room temperature.

The physicochemical properties of AgNPs

UV-Visible (UV-Vis) absorption. The 100x diluted solutions of AgNPs in sterile DI water were prepared to detect the UV-Vis absorption spectroscopy (200 nm-700 nm, 10 nm interval.).

The silver concentration of AgNPs was determined by ICP-OES (inductively coupled plasma optical emission spectroscopy). Briefly, 1 ul of AgNPs was added to 9 ul of 68% concentrated nitric acid to convert silver element into silver ion. Subsequently, 3.99 ml of 1M nitric acid solution was used to dilute the silver ion solution. Thus, 4000-fold diluted solutions of AgNPs were analyzed using ICP-OES.

A series of 10x-100x diluted solutions of AgNPs in sterile DI water (*ca*. 20 μg/ml) were prepared for the determination of hydrated nano size and zeta potential of AgNPs using dynamic light scattering (DLS) (Malvern, Nano-zetasizer).

The morphology and nano size of AgNPs were detected by Transmission electron microscopy (TEM, Philips CM100). Ten microliters of 10x-100x diluted solutions of AgNPs in sterile DI water were deposited onto 400-mid formvor/carbon-coated copper grid. The samples were put on filter paper and dried at room temperature for 1 h, and then images of the AgNPs were captured using TEM.

Antibacterial effect

The minimum inhibitory concentration (MIC) for AgNPs against planktonic *P. gingivilis* was determined using the microdilution method based on the Clinical Laboratory Standards Institute (CLSI) guideline [31]. The maximum test concentration of AgNPs for MIC determination was set to be 2% of the volume of the bacterial suspension. In brief, 100 ul of *P. gingivilis* broth containing serially diluted AgNPs were pipetted into a 96-well cell plate. Subsequently, 10^8 CFU/ml (OD_{660nm} = 0.271–0.279) of *P. gingivilis* in the late logarithmic phase was prepared and inoculated into fresh *P. gingivilis* broth (ratio = 2:100). Then 100 ul of the prepared *P. gingivilis* bacterial suspension (10^6 CFU/ml) was pipetted into the 96-well cell plate and inoculated in an anaerobic incubator at 37℃ for 3 days. Absorbance values at OD_{660nm} were detected to assess the growth of *P. gingivilis*. Negative control and positive controls, including silver diamine fluoride (SDF), $AgNO_3$, and metronidazole (MNZ), were set up parallelly, and three parallel samples and three independent replicates were set up to determine the MIC of AgNPs. The MIC was defined as the lowest concentration that substantially inhibited bacteria growth in the medium.

Time-dependent antibacterial effect of AgNPs

In 96-well cell plate, 200 ul/well of *P. gingivilis* bacterial suspensions (10^6 CFU/ml) were prepared and then shocked by AgNPs at MIC level in an anaerobic incubator at 37℃ for 30 min, 2 h, 6 h, and 24 h. Five microliters of suspension was dropped on blood agar and incubated for 5 days. Three independent assays were performed parallelly. The pictures of blood agar were taken with a camera.

Antibiofilm effect of AgNPs on *P. gingivilis* biofilm

The mature *P. gingivilis* biofilms were incubated in iBidi Cell Plate which was specifically applied for confocal laser scanning microscopy (CLSM). Briefly, 200 ul of *P. gingivilis* suspension (10^8 CFU/ml) in fresh *P. gingivilis* broth was placed in iBidi Cell Plate and incubated in an anaerobic incubator at 37℃ for 6 days (*P. gingivilis* broth was refreshed every 3 days). When the mature *P. gingivilis* biofilms were constructed, we gently discarded the supernatant in the iBidi cell plate and pipetted 200 ul of fresh *P. gingivilis* broth containing AgNPs at MIC and 10*MIC concentration into cells. After an extra 24 h incubation in anaerobic incubator, we removed the supernatant, washed the cells with PBS and stained the biofilm with SYTO9 and PI dyes (Live/Dead bacterial viability kit, ThermoFisher) for 30 min. The fluorescence images were captured by the CLSM.

In addition, the dose-dependent bactericidal effect of AgNPs and P-AgNPs on mature *P. gingivilis* biofilm was detected using CCK8 assay. The mature *P. gingivilis* biofilms were prepared and incubated in 96-well plate. In short, 100 ul of 10% FBS per well was pre-cultured in a sterile 96-well plate for 1 h, 80 rpm at

37℃. After removing the FBS, we added 100 ul of fresh *P. gingivilis* broth containing 1% of *P. gingivilis* suspension (10^8 CFU/ml), incubated the plate in an anaerobic incubator for 6 days at 37℃, and changed the medium every 3 days. Subsequently, we replaced the suspension with fresh medium and performed turbidity measurements at OD600nm (initial value) to confirm the consistency of mature biofilm. Sterile medium containing AgNPs-1/2 and P-AgNPs-1/2 with MIC, 2.5*MIC, 5*MIC, 7.5*MIC and 10*MIC concentrations were freshly prepared at the same time, and were pipetted into the above well plate. After incubation for another 24 hours, the suspension was replaced by fresh medium containing 10% CCK8 and the optical density at 450 nm of well plate were detected in 2 hours. Subsequently, the biofilm was resuspended in 100 ul of fresh medium and incubated on blood agar. CFU below 10 was considered to have no live bacteria.

Cytotoxicity of AgNPs

Human gingival fibroblasts (HGF-1, P6) were used to detect the cytotoxicity of AgNPs. HGF-1 (P3) were resuscitated and passaged in Dulbecco's modified eagle medium (DMEM) containing 10% fetal bovine serum (FBS), 100 U/ml penicillin, and 100 μg/ml streptomycin. Subsequently, 5000 cell/well (P6) were seeded in a 96-well cell plate. After incubation for an additional 24 h for cell attachment, cells were shocked with fresh medium containing MIC concentration of AgNPs for 6 h, 24 h, and 48 h. The medium was then removed and replaced with 90 ul of PrestoBlue Cell viability reagent (10% in PBS, Thermo Fisher.) for 10 min at 37℃. The fluorescence in 560/590nm (excitation/emission) were read by SpectraMax M2 (USA). Five parallel samples and three independent assays were performed.

Statistical analysis

Unless otherwise specified, all the graphs were drawn with GraphPad Prism 5 software. All the data were statistically analyzed using the software SPSS V21.0 (IBM Corporation, Armonk, NY, USA). Normality of data distribution was assessed by Shapiro-Wilk test. Differences between different groups were assessed by t-test and one-way ANOVA with Bonferroni multiple comparison tests. A p-value at or less than 0.05 is statistically significant.

Results

The physicochemical properties of AgNPs-1/2 and P-AgNPs-1/2

AgNPs-1 and AgNPs-2 were successfully synthesized. The UV-Vis absorption spectra detection showed that the peak values of these two AgNPs were 390 nm and 410 nm (Fig. 1). The hydrated nano size was confirmed by DLS (Table 1). The mean and SD values of AgNPs-1 and AgNPs-2 were 15.70±2.26 nm and 24.40±4.16 nm, respectively. TEM image results (Fig. 2) showed a spherical morphology of AgNPs-1/2 and the nano sizes were 17.51±6.12 nm and 23.47±7.57 nm, which were consistent with the results of DLS detection. In addition, the zeta-potential (ζ-potential) of AgNPs-1 detected by DLS was − 36.3 mV, the AgNPs-2 was + 46 mV (Table 1). ICP-OES determined the silver concentration of AgNPs products, they were 0.944 mg/ml and 3.473 mg/ml (Table 1).

The AgNPs-1/2 functionalized by PEG400, PEG2000, PEG-SH5000, PVP, Pluronic P103, P123, F127 were characterized by the above tests as well. The UV-Vis absorption spectrum peaks of all polymer-functionalized AgNPs-1/2 (P-AgNPs-1/2) were between 390nm and 410nm (Fig. 1). The DLS results (Table 1) show that the hydrated particle size of P-AgNPs-1/2 were between 50 nm and 130 nm, which were all larger than the size of AgNPs-1/2. However, the TEM image showed that the particle size of all P-AgNPs remained below 40 nm and did not increase significantly (Fig. 2).

All the P-AgNPs-1 were negatively charges, the ζ-potential were between − 10.7 mV and − 31.9 mV. All the P-AgNPs-2 were positively charges, the ζ-potential were between + 20.2 mV and + 44.0 mV (Table 1). The silver concentration of P-AgNPs-1/2 were 0.302–1.225 mg/ml and 0.171–4.37 mg/ml, respectively (Table 1).

Antibacterial effect of AgNPs-1/2 and P-AgNPs-1/2 on *P. gingivilis* suspension

The MIC values of AgNPs-1/2 and P-AgNPs-1/2 against *P. gingivilis* suspension are shown in Table 1. The MIC value of AgNPs-1/2 were 4.72 μg/ml and 13.89 μg/ml, respectively. Among the AgNPs-1 and P-AgNPs-1 subgroups, only PVP- (MIC: 0.786 μg/ml vs AgNPs-1: 4.72 μg/ml) greatly improved the antibacterial capability of AgNPs-2, and the antibacterial effect of other subgroups was similar to that of AgNPs-1 (MIC: 3.37 to 6.13 μg/ml vs 4.72 μg/ml). Among the AgNPs-2 and P-AgNPs-2 subgroups, all P-AgNPs-2 subgroups significantly improved the antibacterial effect of AgNPs-2 (0.34 to 4.37 μg/ml vs 13.89 μg/ml). P2000- (1.98 μg/ml), PVP- (1.75 μg/ml) and F127- (0.34 μg/ml) greatly improved the antibacterial performance of AgNPs-2.

The time-dependent antibacterial effect of AgNPs was shown in Fig. 3. In AgNPs-1 and P-AgNPs-1 subgroups, P-SH5000- and PVP-AgNPs-1 showed an obvious inhibitory effect at 30 min, P-SH5000- showed complete bactericidal effect at 6 h, and PVP-AgNPs-2 showed complete bactericidal effect at 2 h, similar to the SDF control. F127-AgNPs-2 also showed complete bactericidal effect at 2 h but no effect at 30 min. Other subgroups showed significant inhibitory effect at 2 h and complete bactericidal effect at 24 h, which is similar to the MNZ group. In AgNPs-2 and P-AgNPs-2 subgroups, P400-, P2000-, P-SH5000-, PVP-, P103- and P123- completely inhibited the growth of *P. gingivilis* suspensions at 30 min, which is better than the SDF control group. The AgNPs-2 and F127-AgNPs-2 showed significant inhibitory effect at 30 min and complete bactericidal effect at 2 h which is similar to SDF group.

Antibiofilm effect of AgNPs and p-AgNPs on mature *P. gingivilis* biofilm

The live/dead bacteria staining test results are summarized in Fig. 4. The *P. gingivilis* biofilms were not invaded and destroyed by all AgNPs and P-AgNPs groups at MIC level, barely any red fluorescence representing dead bacteria was detected (data not shown). However, some P-AgNPs-1 and (P-)AgNPs-2 subgroups at 10*MIC level (Fig. 4) were able to kill *P. gingivilis* in biofilm, including PVP-AgNPs-1 (7.8 μg/ml), F127-AgNPs-1 (41.5 μg/ml), AgNPs-2 (138.9 μg/ml) and all P-AgNPs-2 subgroups (3.4 μg/ml-43.7 μg/ml), a large amount of red fluorescence was detected in these subgroups.

In addition, in order to determine the dose-dependent bactericidal effect of the above subgroups against *P. gingivilis* biofilm, the cell viability (CCK8 assay) of AgNPs-2 and P-AgNPs-1/2 subgroups at MIC, 2.5*MIC, 5*MIC, 7.5*MIC and 10*MIC level on *P. gingivilis* biofilm were detected (Fig. 5). The initial value of constructed *P. gingivilis* biofilm at OD_{600nm} was 0.22±0.03 (data not shown. the wells with obvious deviation values were discarded), and no significant difference was detected. A *P. gingivilis* biofilm with consistent growth condition was successfully constructed. Following the AgNPs, SDF, $AgNO_3$ (positive control) and DI water (control) treatment, no significant difference of OD450 value was detected between the (P-)AgNPs-1/2 subgroups and control group at the MIC level, except for the PVP-AgNPs-1 ($P = 0.018$), F127-AgNPs-1 ($P = 0.010$) and F127-AgNPs-2 ($P = 0.034$) subgroups. In the positive control group, SDF at 5*MIC level (45 μg/ml) displayed significant bactericidal effect ($P < 0.001$) compared with the MIC level of SDF, $AgNO_3$ showed a significant bactericidal effect at 10*MIC level (9 μg/ml, $P < 0.001$). In the AgNPs-1 and P-AgNPs-1 subgroups, the PVP-AgNPs-1 (7.86 μg/ml) and F127-AgNPs-1 (41.50 μg/ml) showed a significant bactericidal effect ($P = 0.002$ and 0.011) at 10*MIC level compared with the MIC level. In the AgNPs-2 and P-AgNPs-2 subgroups, the AgNPs-2 at 5*MIC (69.45 μg/ml) to 10*MIC level (138.9 μg/ml, $P < 0.001$) showed a significant bactericidal effect ($P < 0.001$). The P400-AgNPs-2 had a significant bactericidal effect at 2.5*MIC level (10.93 μg/ml, $P < 0.001$), and more significant bactericidal effect ($OD_{450nm} < 0.10$) was demonstrated at 5*MIC level (21.85 μg/ml, $P < 0.001$). The P2000-AgNPs-2 (14.87 μg/ml, $P < 0.001$), P103-AgNPs-2 (31.14 μg/ml, $P < 0.001$) and P123-AgNPs-2 (21.27 μg/ml, $P < 0.001$) showed significant bactericidal effects at 7.5*MIC. P-SH5000-AgNPs-2 (25.60 μg/ml, $P < 0.001$), PVP-AgNPs-2 (17.50 μg/ml, $P < 0.001$), and F127-AgNPs-2 (3.43 μg/ml, $P = 0.001$) showed significant bactericidal effects at 10*MIC. However, although the $AgNO_3$, PVP-AgNPs-1, F127-AgNPs-1 and AgNPs-2 showed significant bactericidal effects at 10*MIC, their OD_{450nm} values were over 0.10. Resuspensions of these biofilms were incubated in blood agar to determine the presence of viable bacteria. The results showed that over 85 CFUs were detected on the blood agar in the $AgNO_3$, F127-AgNPs-1, and AgNPs-2 subgroups, but very few colonies (< 6) were detected in other subgroups (data not shown). In summary, the order of the complete bactericidal values of these AgNPs subgroups is: F127-AgNPs-3 (3.425 μg/ml) < PVP-AgNPs-2 (7.86 μg/ml) < P2000-AgNPs-3 (14.865 μg/ml) < PVP-AgNPs-3 (17.5 μg/ml) < P123-AgNPs-3 (21.27 μg/ml) < P400-AgNPs-3 (21.85 μg/ml) < P-SH5000-AgNPs-3 (25.6 μg/ml) < P103-AgNPs-3 (31.14 μg/ml) < SDF (45 μg/ml), and undetermined AgNO3 (> 9 μg/ml) < F127-AgNPs-2 (> 41.5 μg/ml) < AgNPs-3 (> 138.9 μg/ml).

Cytotoxicity of AgNPs and p-AgNPs on HGF

Cytotoxicity assay results of AgNPs and P-AgNPs on HGF are displayed in Fig. 6. At MIC level, no significant cytotoxic effects were detected in AgNPs-1 and P-AgNPs-1 subgroups compared with control groups. However, in AgNPs-2 and P-AgNPs-2 groups, P400- and P123- subgroups displayed significant cytotoxicity in 6 hours ($P < 0.001$), and cytotoxicity of P400- appeared as early as 30 min (data not shown). P2000-, P-SH5000- and P103- subgroups ($P = 0.006$, 0.035, 0.009 respectively) also displayed significant cytotoxic effect at 6 h, which were significantly weaker than that of P400- and P123-

subgroups, but not at 24 h and 48 h. AgNPs-2, F123-AgNPs-2, and F127-AgNPs-2 ($P < 0.001$, $P = 0.023$, $P < 0.001$) displayed significant cytotoxic effects at 48 h.

Discussion

In the present study, AgNPs and P-AgNPs with spherical morphology, sizes ranging from 10 nm to 50 nm, but opposite surface charges were successfully synthesized and confirmed by UV-Vis absorption, DLS and TEM. Results of the comparative analysis show the physical properties of AgNPs-1/2 are not significantly altered by polymer functionalized, but the surface chemical properties are modified which have a significant impact on the biological properties of AgNPs-1/2. However, not all the polymer-functionalization can improve these biological properties,

Regarding the physical properties, the complementary combined use of UV-Vis, DLS, and TEM in the present study confirmed the nano dimension and spherical structure of AgNPs and P-AgNPs [32]. The peak values of all AgNPs and P-AgNPs detected by UV-Vis were between 390 nm and 410 nm, which is the characteristic plasmon resonance absorption peak of typical spherical silver nanoparticles [33]. The hydrated nano size of P-AgNPs detected by DLS increased significantly by more than 25 nm (50–130 nm). However, the TEM results show the dimension of all P-AgNPs-1/2 nanoparticles is between 10–40 nm. This indicates that the dimension of P-AgNPs particles does not increase significantly while the increased hydrated size is associated with the coating of polymer. In the TEM image of PVP-AgNPs-1, we captured some 50–80 nm AgNPs with halo. This may be caused by the coating of PVP after AgNPs aggregation which involves Ostwald ripening phenomenon [34]. The comparative analysis of the hydrated size of AgNPs-1/2 and P-AgNPs-1/2 shows the degree of increase in hydrated particle size is not consistent with the molecular weight of polymer. Chauhan et al. found that this may be relate to the efficiency of polymer adsorption on the surface of AgNPs [35]. Hence, the increase in the nano size of P-SH5000 and PVP indicates that they have strong adsorption to AgNPs. To summarize, polymer functionalization does not significantly alter the physical dimension of nanoparticles.

In addition, polymer functionalization has no influence on the surface charge properties of AgNPs-1/2 but affects the surface charge value (ζ-potential value). In general, the ζ-potential of a solution is an indicator of the stability of colloidal dispersions and a solution with an absolute value over 20 is considered stable and dispersed [32]. Hence, the AgNPs-1/2 in this study were stable solutions but the incorporation of polymer seems to negatively influence the stability of AgNPs, especially PEG400-AgNPs-1. To assess the stability of AgNPs, we conducted continuous observation and UV-Vis test at the 28th week. Only AgNPs-2 showed visible agglomeration and precipitation at the 16th week, even though its original ζ-potential was + 46. All other AgNPs and (P-)AgNPs were still spherical nanoparticles at the 28th week (390-410nm. data not show). This indicates that polymer functionalization improves the stability of the positively charged AgNPs, and does not affect the stability of the negatively charged AgNPs within 28 weeks. However, since ζ-potential value is related to the concentration of solution [32, 36], the detected value only reflects the stability of the diluted AgNPs solution to a certain extent. Therefore, we suggest to combine the ζ-

potential test and other tests, such as UV-Vis, in longitudinal observations to evaluate the stability of AgNPs.

Many researches have shown that the nanometer size [37], surface charge [38, 39] and surface chemical [18, 20, 23, 40] of AgNPs are related to their antibacterial property. In the present study, the negative correlation between nano size and antibacterial capability was confirmed only in AgNPs-1 and AgNPs-2 without polymer functionalization. This indicates that after polymer functionalization, the modified surface chemical property, rather than particle dimension, is the priority/primary effect on the antibacterial property [18, 20, 23, 40]. In addition, the positively charged AgNPs, especially polymer-functionalized AgNPs in the current study, generally exhibited stronger antibacterial activity than the negatively charged AgNPs over a short period of time. This is highly correlated with the electrostatic interactions between positively charged materials and the negatively charged surfaces of bacteria [41]. However, in the present study the negatively charged AgNPs undergoing polymer functionalization, such as with PVP, also exhibited similar or even better antibacterial activity. We speculate that this results from the modification of surface chemistry. PVP has good affinity on cell membrane and cytoplasm [42], and it increases the connection between membrane and AgNPs through other chemical bonds or synergy effects [43], thereby increasing the chance of silver attaching to cells. The specific mechanism remains to be explored further in future studies.

Since bacterial biofilm plays a more important role in human health and disease than suspended bacteria [44, 45], it is more important to evaluate the antibiofilm effect of AgNPs. It has been found that the initial partition of AgNPs on biofilm interface is controlled by electrostatic interaction [46]. This explains why all the positively charged AgNPs and P-AgNPs in the present study displayed good bactericidal effect against *P. gingivilis* biofilm. This kind of electrostatic interaction enhances the attachment of AgNPs and further causes alteration of cell permeability, leading to leakage of intracellular components and cell death [46, 47]. In addition, the negatively charged AgNPs in the present study, i.e. PVP-AgNPs-1 and F127-AgNPs-1, also showed a significant antibiofilm effect against *P. gingivilis* biofilm. We speculate that the enhanced attachment of AgNPs to cells exerts a crucial role in the antibiofilm process as both PVP and F127 have good affinity for cells [42, 48]. That is to say, enhancing the attachment of AgNPs on cell membrane by electrostatic interaction or surface chemical modification is an effective method to improve the antibiofilm activity of AgNPs [49].

Cytotoxicity is another aspect that needs to be evaluated before clinical application of AgNPs. Previous studies reported that the cytotoxicity of AgNPs is associated with many factors, including nanoparticle dimension, shape, surface charge and surface chemical [50–53]. In the present study, surface charge and surface chemical were the only two variables studied, both of which are risk factors affecting the cytotoxicity of AgNPs. The positively charged AgNPs in the present study have higher cytotoxicity and after polymer functionalization, most positively charged AgNPs displayed more obvious cytotoxicity. According to the known action mechanism of AgNPs [54, 55], both the initial attachment of AgNPs to cell membrane and the following release of Ag^+ ions influence their cytotoxicity, including the subsequent intracellular penetration, reactive oxygen species (ROS), free radical generation, DNA damage and protein

denaturation [53, 56]. Hence, both electrostatic interaction and surface chemical modification can enhance the attachment of AgNPs on cell membrane and cellular uptake, resulting in stronger cytotoxicity [7, 57]. However, there are also polymer functionalization in the present study, such as using PVP, which did not increase the cytotoxicity of positively charged AgNPs. We speculate that this is related to the low treatment concentration of PVP-AgNPs-2. Based on the 'Trojan-horse' mechanism, it is postulated that the cytotoxicity of AgNPs is associated with the release of toxic ions in intracellular environments, and both intracellular ROS and acidic condition of lysosomal cellular compartment can induce the reaction with AgNPs to form more Ag^+ ions [58, 59]. This mechanism supports that the cytotoxicity of AgNPs is dose-dependent involving the release of Ag^+ ions [54, 55]. Low doses of silver reduce cytotoxicity by inducing protective autophagy in cells [60]. However, the F127-AgNPs-2 in the present study, which is the lowest treatment concentration subgroup, showed cytotoxicity at 48 h. We attribute this to the surface chemical modification caused by the F127 polymer which affects the attachment, release and accumulation of silver on the cell surface, thereby causing long-term cytotoxicity. In summary, the lower the treatment concentration of AgNPs, the greater the potential for low cytotoxicity is, and the surface chemical also has a significant effect.

It should be noted that none of the AgNPs in the present study showed no cytotoxicity at concentrations capable of exerting antibiofilm activity. All the positively/negatively charged AgNPs and P-AgNPs showed significant cytotoxicity on HGF at concentrations higher than 2.5* MIC (data not shown). We speculate that there is a certain positive correlation between the antibacterial capability of AgNPs and its cytotoxicity. Khalil et al. also found that the antibacterial material with lower MIC value in their study exhibited higher cytotoxicity [61]. Hence, we should find a balance point between antibacterial and cytotoxicity of antibacterial materials for application. Besides, we should not ignore the synthesis method of AgNPs, because some green synthesized AgNPs show better biocompatibility [62]. In summary, before suggesting for clinical application, further investigation on how to reduce the cytotoxicity of (P-)AgNPs at the antibiofilm concentration level is needed.

Conclusion

Polymer functionalization, as carried out in the present study, only minimally alters the physical properties of AgNPs, including nano-size and surface charge, but modifies their surface chemical properties which are closely related to their biological property. The antibacterial, antibiofilm properties and cytotoxicity of AgNPs can be significantly optimized to varying degrees by some polymer functionalization, especially using PVP, depending on surface charge. However, none of the AgNPs studied has low cytotoxicity at the antibiofilm concentration levels.

Abbreviations

AgNPs, silver nanoparticles; P-AgNPs, polymer-functionalized AgNPs; UV-Vis, ultraviolet-visible; DLS, dynamic light scattering; TEM, transmission electron microscopy; ICP-OES, inductively coupled plasma optical emission spectroscopy; CLSM, confocal laser scanning microscope; MIC, minimize inhibitory

concentration; SDF, silver diamine fluoride; MNZ, metronidazole; HGF, human gingival fibroblast; PVP, polyvinylpyrrolidone; CFU, colony forming unit.

Declarations

Ethics approval and consent to participate: Not applicable

Consent for publication: Not applicable

Availability of data and materials: The datasets used and/or analyzed during the current study are available from the corresponding author on reasonable request.

Competing interests: The authors declare that they have no competing interests.

Funding: This work was financially supported by the grants from the Tam Wah-ching Endowed Professorship in Hong Kong.

Authors' contributions: MZ conceived the project, performed the entire experiment, analyzed and interpreted the data, and was a major contributor in writing the manuscript. EL conceived the project, analyzed and interpreted the data, and revised the manuscript. All authors read and approved the final manuscript.

Acknowledgments: The authors would like to acknowledge Prof Leung Wai Keung from the University of Hong Kong for providing HGF, and Xuan Li, Ting Zou, and Tianfan Cheng for technical support.

References

1. Barras F, Aussel L, Ezraty B. **Silver and Antibiotic, New Facts to an Old Story**. Antibiotics (Basel, Switzerland) 2018, 7(3).
2. Bhattacharya R, Mukherjee P. Biological properties of "naked" metal nanoparticles. Adv Drug Deliv Rev. 2008;60(11):1289–306.
3. Chernousova S, Epple M. **Silver as Antibacterial Agent: Ion, Nanoparticle, and Metal**. 2013, 52(6):1636–1653.
4. Konop M, Damps T, Misicka A, Rudnicka L. Certain Aspects of Silver and Silver Nanoparticles in Wound Care: A Minireview. J Nanomaterials. 2016;2016:7614753.
5. Rai MK, Deshmukh SD, Ingle AP, Gade AK. Silver nanoparticles: the powerful nanoweapon against multidrug-resistant bacteria. J Appl Microbiol. 2012;112(5):841–52.
6. Chen X, Schluesener HJ. Nanosilver: a nanoproduct in medical application. Toxicol Lett. 2008;176(1):1–12.

7. Malysheva A, Ivask A, Doolette CL, Voelcker NH, Lombi E. Cellular binding, uptake and biotransformation of silver nanoparticles in human T lymphocytes. Nat Nanotechnol. 2021;16(8):926–32.
8. Lok C-N, Ho C-M, Chen R, He Q-Y, Yu W-Y, Sun H, Tam PK-H, Chiu J-F, Che C-M. Proteomic Analysis of the Mode of Antibacterial Action of Silver Nanoparticles. J Proteome Res. 2006;5(4):916–24.
9. Makvandi P, Iftekhar S, Pizzetti F, Zarepour A, Zare EN, Ashrafizadeh M, Agarwal T, Padil VVT, Mohammadinejad R, Sillanpaa M, et al. Functionalization of polymers and nanomaterials for water treatment, food packaging, textile and biomedical applications: a review. Environ Chem Lett. 2021;19(1):583–611.
10. Xiu ZM, Zhang QB, Puppala HL, Colvin VL, Alvarez PJ. Negligible particle-specific antibacterial activity of silver nanoparticles. Nano Lett. 2012;12(8):4271–5.
11. Dakal TC, Kumar A, Majumdar RS, Yadav V. Mechanistic Basis of Antimicrobial Actions of Silver Nanoparticles. Front Microbiol. 2016;7:1831.
12. Huma ZE, Javed I, Zhang Z, Bilal H, Sun Y, Hussain SZ, Davis TP, Otzen DE, Landersdorfer CB, Ding F, et al. Nanosilver Mitigates Biofilm Formation via FapC Amyloidosis Inhibition. Small. 2020;16(21):e1906674.
13. Hajtuch J, Hante N, Tomczyk E, Wojcik M, Radomski MW, Santos-Martinez MJ, Inkielewicz-Stepniak I. Effects of functionalized silver nanoparticles on aggregation of human blood platelets. Int J Nanomedicine. 2019;14:7399–417.
14. Bryaskova R, Pencheva D, Nikolov S, Kantardjiev T. Synthesis and comparative study on the antimicrobial activity of hybrid materials based on silver nanoparticles (AgNps) stabilized by polyvinylpyrrolidone (PVP). J Chem Biol. 2011;4(4):185–91.
15. Rolim WR, Pieretti JC, Renó DLS, Lima BA, Nascimento MHM, Ambrosio FN, Lombello CB, Brocchi M, de Souza ACS, Seabra AB. Antimicrobial Activity and Cytotoxicity to Tumor Cells of Nitric Oxide Donor and Silver Nanoparticles Containing PVA/PEG Films for Topical Applications. ACS Appl Mater Interfaces. 2019;11(6):6589–604.
16. Tepale N, Fernández-Escamilla VVA, Flores-Aquino E, Sánchez-Cantú M, Luna-Flores A, González-Coronel VJ. Use of Pluronic P103 Triblock Copolymer as Structural Agent during Synthesis of Hybrid Silver Nanoparticles. J Nanomaterials. 2019;2019:9384072.
17. Zhao R, Lv M, Li Y, Sun M, Kong W, Wang L, Song S, Fan C, Jia L, Qiu S, et al. Stable Nanocomposite Based on PEGylated and Silver Nanoparticles Loaded Graphene Oxide for Long-Term Antibacterial Activity. ACS Appl Mater Interfaces. 2017;9(18):15328–41.
18. Tiwari V, Tiwari M, Solanki V. Polyvinylpyrrolidone-Capped Silver Nanoparticle Inhibits Infection of Carbapenem-Resistant Strain of Acinetobacter baumannii in the Human Pulmonary Epithelial Cell. Front Immunol. 2017;8:973.
19. Selvakumar P, Sithara R, Viveka K, Sivashanmugam P. Green synthesis of silver nanoparticles using leaf extract of Acalypha hispida and its application in blood compatibility. J Photochem photobiology B Biology. 2018;182:52–61.

20. Barrios-Gumiel A, Sanchez-Nieves J, Pérez-Serrano J, Gómez R, de la Mata FJ. PEGylated AgNP covered with cationic carbosilane dendrons to enhance antibacterial and inhibition of biofilm properties. Int J Pharm. 2019;569:118591.
21. Alexandridis P, Alan Hatton T. Poly(ethylene oxide) poly(propylene oxide) poly(ethylene oxide) block copolymer surfactants in aqueous solutions and at interfaces: thermodynamics, structure, dynamics, and modeling. Colloids Surf A. 1995;96(1):1–46.
22. Lin SY, Kawashima Y. The influence of three poly(oxyethylene)poly(oxypropylene) surface-active block copolymers on the solubility behavior of indomethacin. Pharm Acta Helv. 1985;60(12):339–44.
23. dos Santos CA, Jozala AF, Pessoa A Jr, Seckler MM. Antimicrobial effectiveness of silver nanoparticles co-stabilized by the bioactive copolymer pluronic F68. J Nanobiotechnol. 2012;10:43.
24. Liu T, Aman A, Ainiwaer M, Ding L, Zhang F, Hu Q, Song Y, Ni Y, Tang X. Evaluation of the anti-biofilm effect of poloxamer-based thermoreversible gel of silver nanoparticles as a potential medication for root canal therapy. Sci Rep. 2021;11(1):12577.
25. D'Aiuto F, Gkranias N, Bhowruth D, Khan T, Orlandi M, Suvan J, Masi S, Tsakos G, Hurel S, Hingorani A, et al: **Systemic effects of periodontitis treatment in patients with type 2 diabetes**: **a 12 month**, **single-centre**, **investigator-masked**, **randomised trial**. *The lancet Diabetes endocrinology* 2018, **6**(12):954–965.
26. Park S, Kim S, Kang S, Yoon C, Lee H, Yun P, Youn T, Chae I. Improved oral hygiene care attenuates the cardiovascular risk of oral health disease: a population-based study from Korea. Eur Heart J. 2019;40(14):1138–45.
27. Bulgart H, Neczypor E, Wold L, Mackos A. Microbial involvement in Alzheimer disease development and progression. Mol neurodegeneration. 2020;15(1):42.
28. Khadka S, Khan S, King A, Goldberg L, Crocombe L, Bettiol S. Poor oral hygiene, oral microorganisms and aspiration pneumonia risk in older people in residential aged care: a systematic review. Age ageing. 2021;50(1):81–7.
29. Frank AJ, Cathcart N, Maly KE, Kitaev V. Synthesis of Silver Nanoprisms with Variable Size and Investigation of Their Optical Properties: A First-Year Undergraduate Experiment Exploring Plasmonic Nanoparticles. J Chem Educ. 2010;87(10):1098–101.
30. Abbaszadegan A, Nabavizadeh M, Gholami A, Aleyasin ZS, Dorostkar S, Saliminasab M, Ghasemi Y, Hemmateenejad B, Sharghi H. **Positively charged imidazolium-based ionic liquid-protected silver nanoparticles: a promising disinfectant in root canal treatment**. 2015, 48(8):790–800.
31. MA P, DJ D. Progress in antifungal susceptibility testing of Candida spp. by use of Clinical and Laboratory Standards Institute broth microdilution methods, 2010 to 2012. J Clin Microbiol. 2012;50(9):2846–56.
32. Mourdikoudis S, Pallares RM, Thanh NTK. Characterization techniques for nanoparticles: comparison and complementarity upon studying nanoparticle properties. Nanoscale. 2018;10(27):12871–934.
33. Udaya Bhaskara Rao T, Pradeep T. Luminescent Ag7 and Ag8 Clusters by Interfacial Synthesis. Angew Chem Int Ed. 2010;49(23):3925–9.

34. Chen M, Feng YG, Wang X, Li TC, Zhang JY, Qian DJ. Silver nanoparticles capped by oleylamine: formation, growth, and self-organization. Langmuir. 2007;23(10):5296–304.
35. Chauhan PS, Kumarasamy M, Sosnik A, Danino D. Enhanced Thermostability and Anticancer Activity in Breast Cancer Cells of Laccase Immobilized on Pluronic-Stabilized Nanoparticles. ACS Appl Mater Interfaces. 2019;11(43):39436–48.
36. Baldassarre F, Cacciola M, Ciccarella G. **A predictive model of iron oxide nanoparticles flocculation tuning Z-potential in aqueous environment for biological application**. Journal of Nanoparticle Research 2015, 17.
37. Raza MA, Kanwal Z, Rauf A, Sabri AN, Riaz S, Naseem S. **Size- and Shape-Dependent Antibacterial Studies of Silver Nanoparticles Synthesized by Wet Chemical Routes**. 2016, 6(4):74.
38. Abbaszadegan A, Ghahramani Y, Gholami A, Hemmateenejad B, Dorostkar S, Nabavizadeh M, Sharghi H. The Effect of Charge at the Surface of Silver Nanoparticles on Antimicrobial Activity against Gram-Positive and Gram-Negative Bacteria: A Preliminary Study. J Nanomaterials. 2015;2015:720654.
39. Gottenbos B, Grijpma DW, van der Mei HC, Feijen J, Busscher HJ. Antimicrobial effects of positively charged surfaces on adhering Gram-positive and Gram-negative bacteria. J Antimicrob Chemother. 2001;48(1):7–13.
40. IX Y, IS Z, ML M, ECM L, J T, LY QL. S, CH C: Synthesis and Characterization of Fluoridated Silver Nanoparticles and Their Potential as a Non-Staining Anti-Caries Agent. Int J Nanomed. 2020;15:3207–15.
41. Wilhelm MJ, Sharifian Gh M, Chang CM, Wu T, Li Y, Ma J, Dai HL. **Determination of Bacterial Surface Charge Density Via Saturation of Adsorbed Ions**. *bioRxiv* 2020:2020.2009.2029.318840.
42. Rackur H: **New aspects of mechanism of action of povidone-iodine**. *The Journal of hospital infection* 1985, **6 Suppl A**:13–23.
43. Jena G, Sofia S, Anandkumar B, Vanithakumari SC, George RP, Philip J. Graphene oxide/polyvinylpyrrolidone composite coating on 316L SS with superior antibacterial and anti-biofouling properties. Prog Org Coat. 2021;158:106356.
44. Vestby LK, Grønseth T, Simm R, Nesse LL. **Bacterial Biofilm and its Role in the Pathogenesis of Disease**. Antibiotics (Basel, Switzerland) 2020, 9(2).
45. Jamal M, Ahmad W, Andleeb S, Jalil F, Imran M, Nawaz MA, Hussain T, Ali M, Rafiq M, Kamil MA. Bacterial biofilm and associated infections. J Chin Med Association: JCMA. 2018;81(1):7–11.
46. Desmau M, Gélabert A, Levard C, Ona-Nguema G, Vidal V, Stubbs JE, Eng PJ, Benedetti MF: **Dynamics of silver nanoparticles at the solution/biofilm/mineral interface**. *Environmental Science: Nano* 2018, **5**(10):2394–2405.
47. Rabea EI, Badawy MET, Stevens CV, Smagghe G, Steurbaut W. Chitosan as antimicrobial agent: applications and mode of action. Biomacromolecules. 2003;4(6):1457–65.
48. Khattak SF, Bhatia SR, Roberts SC. Pluronic F127 as a cell encapsulation material: utilization of membrane-stabilizing agents. Tissue Eng. 2005;11(5–6):974–83.

49. Kumariya R, Sood SK, Rajput YS, Saini N, Garsa AK. Increased membrane surface positive charge and altered membrane fluidity leads to cationic antimicrobial peptide resistance in Enterococcus faecalis. Biochim et Biophys Acta (BBA) - Biomembr. 2015;1848(6):1367–75.
50. Silva T, Pokhrel LR, Dubey B, Tolaymat TM, Maier KJ, Liu X. Particle size, surface charge and concentration dependent ecotoxicity of three organo-coated silver nanoparticles: Comparison between general linear model-predicted and observed toxicity. Sci Total Environ. 2014;468–469:968–76.
51. Gliga AR, Skoglund S, Wallinder IO, Fadeel B, Karlsson HL. Size-dependent cytotoxicity of silver nanoparticles in human lung cells: the role of cellular uptake, agglomeration and Ag release. Part Fibre Toxicol. 2014;11:11.
52. Pang C, Brunelli A, Zhu C, Hristozov D, Liu Y, Semenzin E, Wang W, Tao W, Liang J, Marcomini A, et al. Demonstrating approaches to chemically modify the surface of Ag nanoparticles in order to influence their cytotoxicity and biodistribution after single dose acute intravenous administration. Nanotoxicology. 2016;10(2):129–39.
53. El Badawy AM, Silva RG, Morris B, Scheckel KG, Suidan MT, Tolaymat TM. Surface charge-dependent toxicity of silver nanoparticles. Environ Sci Technol. 2011;45(1):283–7.
54. Pareek V, Gupta R, Panwar J. Do physico-chemical properties of silver nanoparticles decide their interaction with biological media and bactericidal action? A review. Mater Sci Eng C Mater Biol Appl. 2018;90:739–49.
55. Liao C, Li Y, Tjong SC. **Bactericidal and Cytotoxic Properties of Silver Nanoparticles**. Int J Mol Sci 2019, 20(2).
56. Nguyen KC, Richards L, Massarsky A, Moon TW, Tayabali AF. Toxicological evaluation of representative silver nanoparticles in macrophages and epithelial cells. Toxicol In Vitro. 2016;33:163–73.
57. Treuel L, Brandholt S, Maffre P, Wiegele S, Shang L, Nienhaus GU. Impact of protein modification on the protein corona on nanoparticles and nanoparticle-cell interactions. ACS Nano. 2014;8(1):503–13.
58. Hsiao IL, Hsieh YK, Wang CF, Chen IC, Huang YJ. Trojan-horse mechanism in the cellular uptake of silver nanoparticles verified by direct intra- and extracellular silver speciation analysis. Environ Sci Technol. 2015;49(6):3813–21.
59. Sabella S, Carney RP, Brunetti V, Malvindi MA, Al-Juffali N, Vecchio G, Janes SM, Bakr OM, Cingolani R, Stellacci F, et al. A general mechanism for intracellular toxicity of metal-containing nanoparticles. Nanoscale. 2014;6(12):7052–61.
60. Li H, Chen J, Fan H, Cai R, Gao X, Meng D, Ji Y, Chen C, Wang L, Wu X. Initiation of protective autophagy in hepatocytes by gold nanorod core/silver shell nanostructures. Nanoscale. 2020;12(11):6429–37.
61. Khalil WA, Sherif HHA, Hemdan BA, Khalil SKH, Hotaby WE. Biocompatibility enhancement of graphene oxide-silver nanocomposite by functionalisation with polyvinylpyrrolidone. IET Nanobiotechnol. 2019;13(8):816–23.

62. Selvakumar P, Sithara R, Viveka K, Sivashanmugam P. Green synthesis of silver nanoparticles using leaf extract of Acalypha hispida and its application in blood compatibility. J Photochem Photobiol B. 2018;182:52–61.

Tables

Table 1. Summary of the nano size, zeta-potential (DLS), silver concentration (ICP-OES), and MIC values for AgNPs-1/2 and P-AgNPs-1/2.

Code			Size			Zeta-potential		AgNPs concentration (mg/ml)	MIC (µg/ml)
			mean (d.nm)	SD	PDI	mean (mV)	SD		
SDF									9.00
AgNO3									0.90
Metronidazole									0.13
AgNPs-1			15.7	2.256	0.149	-35.0	3.170	0.944	4.72
	a-	PEG400	50.8	2.783	0.242	-10.7	0.700	0.302	6.03
	b-	PEG2000	105.7	1.708	0.471	-30.5	1.150	1.225	6.13
	c-	PEG-SH 5000	105.7	3.190	0.384	-18.0	0.702	1.077	3.37
	d-	PVP	122.4	2.219	0.256	-19.6	0.833	1.179	0.79
	e-	P103	78.8	0.760	0.419	-31.9	5.450	0.728	4.86
	f-	P123	73.0	0.331	0.393	-31.5	6.650	0.711	3.56
	g-	F127	105.7	10.340	0.273	-28.6	0.265	0.623	4.15
AgNPs-2			24.4	4.158	0.300	46.0	4.440	3.473	13.89
	a-	PEG400	117.4	3.365	0.379	25.7	0.929	4.370	4.37
	b-	PEG2000	68.1	2.986	0.264	38.1	1.460	0.991	1.98
	c-	PEG-SH 5000	122.4	5.164	0.310	20.2	2.690	2.560	2.56
	d-	PVP	105.7	2.420	0.345	27.4	0.967	1.750	1.75
	e-	P103	58.8	1.050	0.240	22.5	3.700	2.076	4.15
	f-	P123	50.8	9.646	0.198	44.0	0.971	1.418	2.84
	g-	F127	58.8	1.018	0.269	28.7	2.790	0.171	0.34

SDF, silver diamine fluoride. SD, standard deviation. PDI, polydispersity index. MIC, minimum inhibitory concentration.

Scheme

Scheme 1 is available in the Supplementary Files section.

Figures

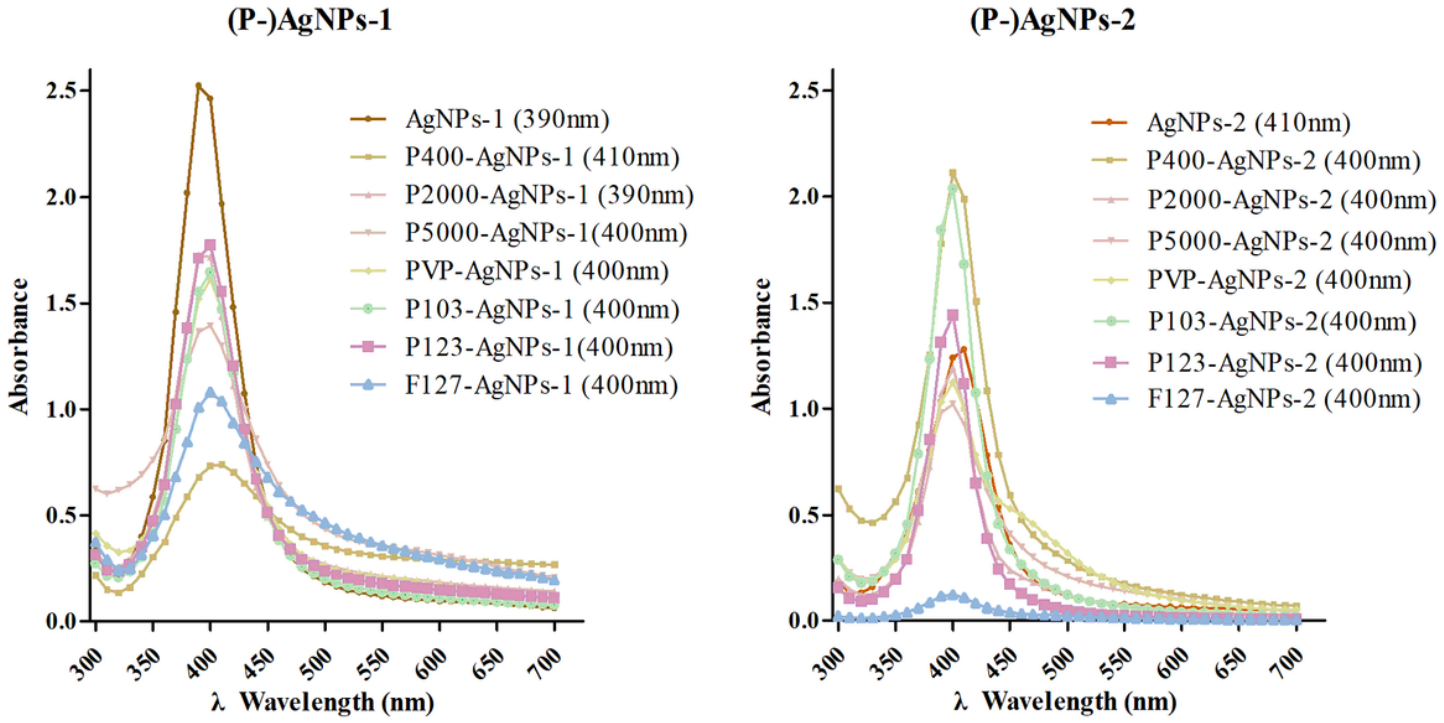

Figure 1

The UV-Vis absorption spectroscopy detection of AgNPs-1/2 and P-AgNPs-1/2. In parentheses is the peak value of the samples.

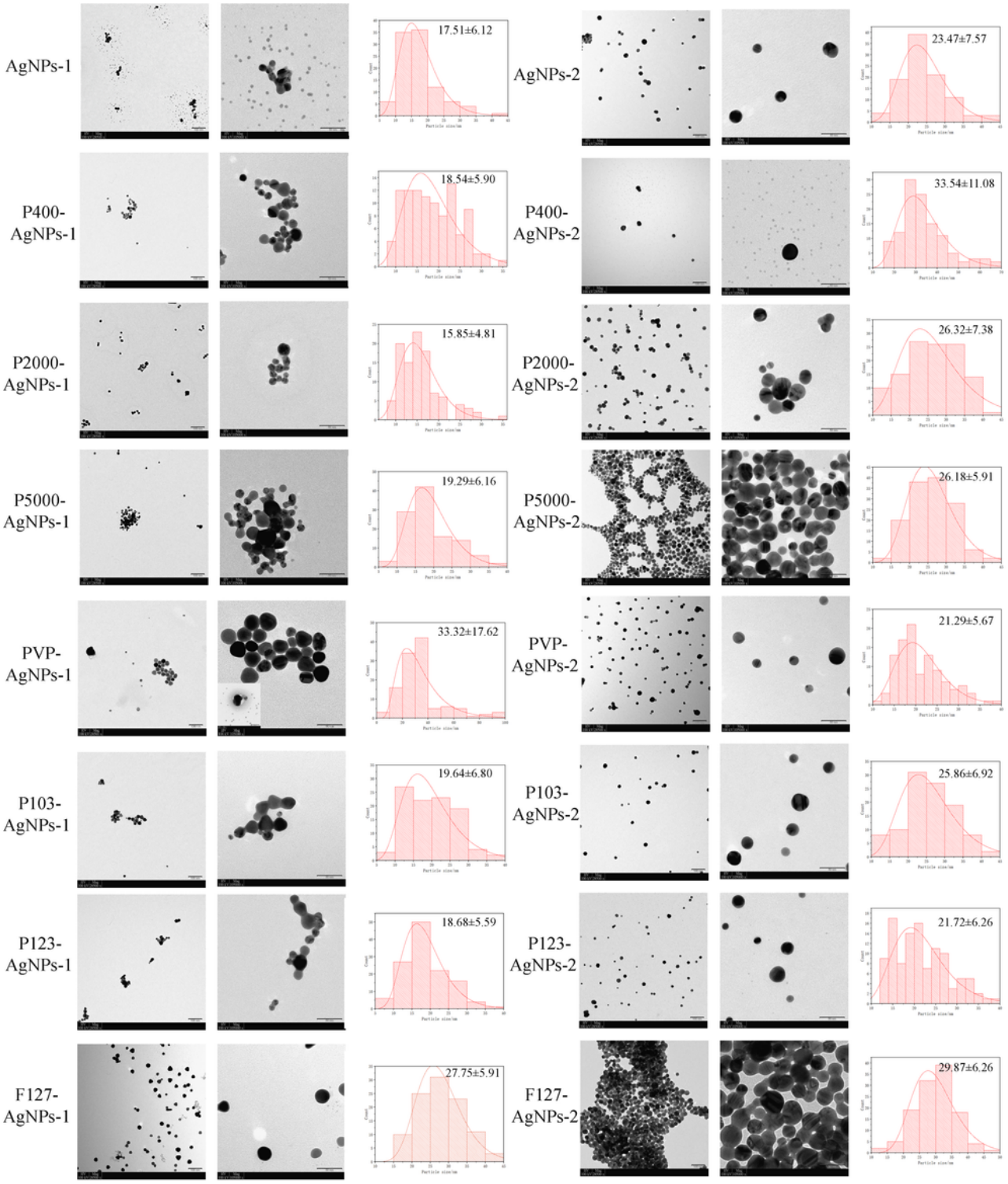

Figure 2

TEM images of AgNPs-1/2 and P-AgNPs-1/2, along with the histograms of nanometer size distribution (ImageJ).

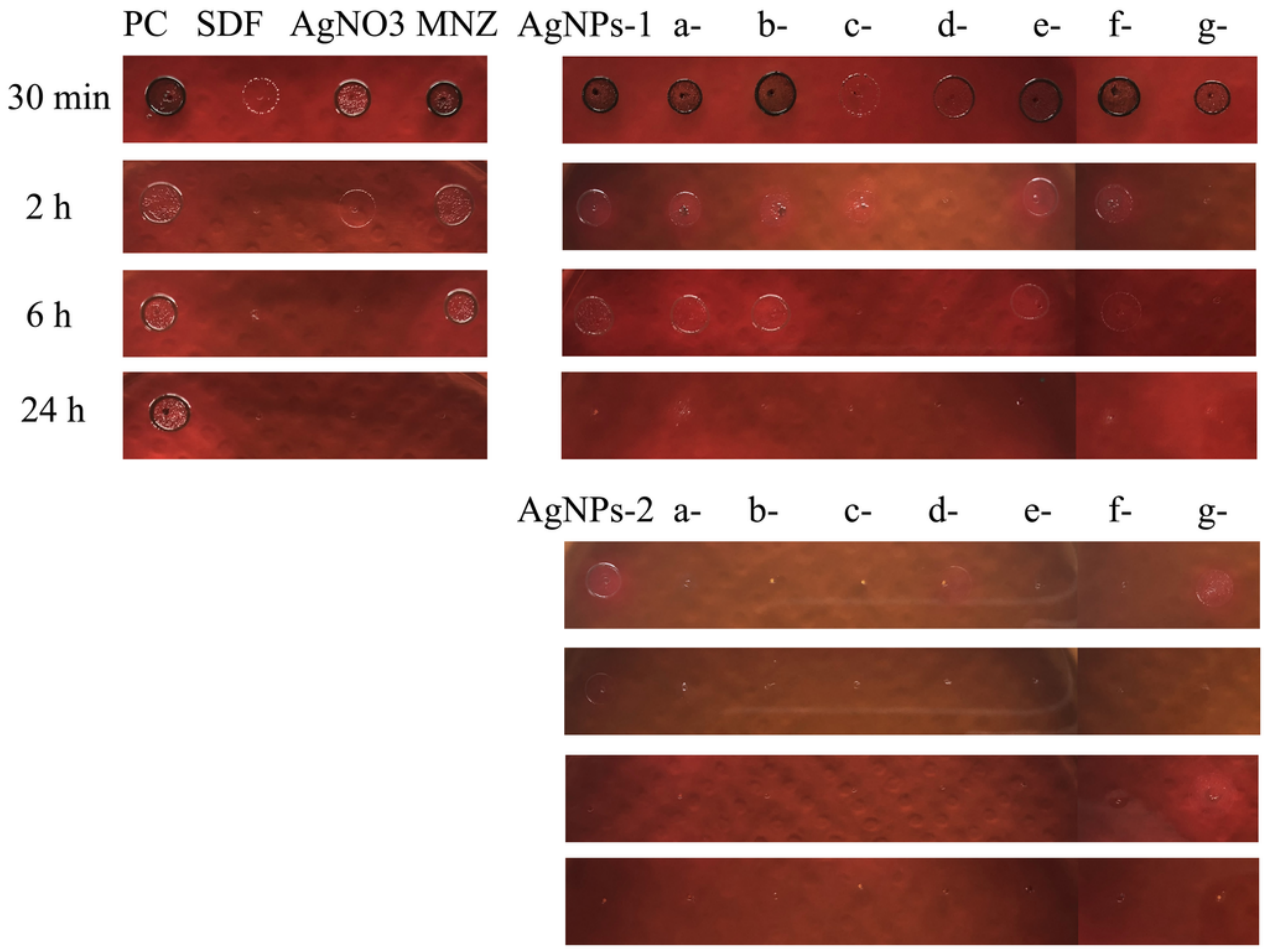

Figure 3

Summary for the time-dependent antibacterial effect of AgNPs-1/2 and P-AgNPs-1/2 on *P. gingivilis* suspensions. a, b, c, d, e, f, and g are PEG 400, PEG 2000, PEG-SH 5000, PVP (MW 10000), Pluronic P103 (Mn 5000), P123 (Mn 5800), and F127 (Mn 12000), respectively. SDF, silver diamine fluoride. MNZ, metronidazole.

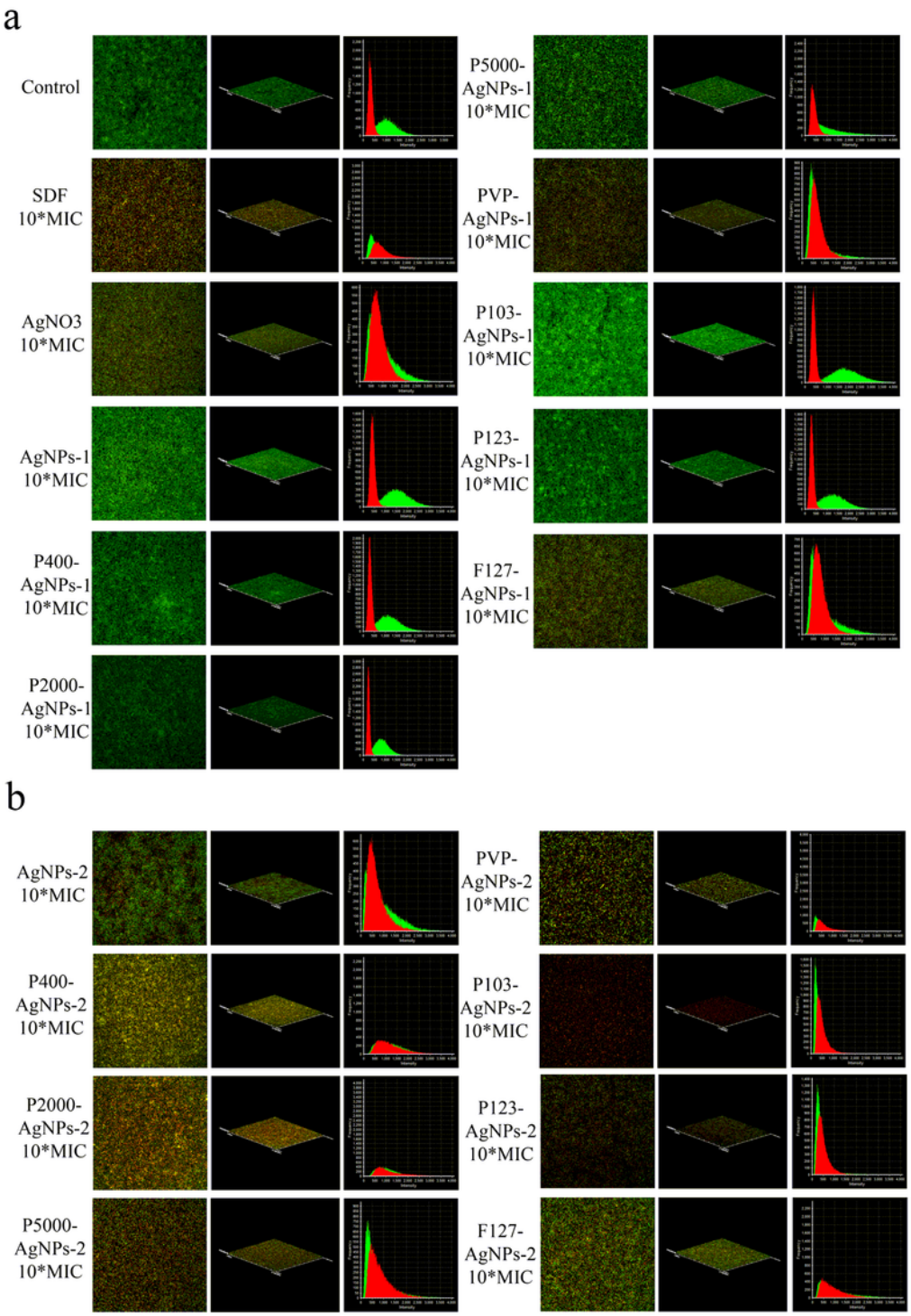

Figure 4

CLSM images showing the antibiofilm effect of AgNPs-1/2 and P-AgNPs-1/2 on *P. gingivilis* biofilm (Live/Dead bacterial viability kit), including merged images, 3D models, and intensity-frequency area graphs. Red for dead bacteria and green for live bacteria.

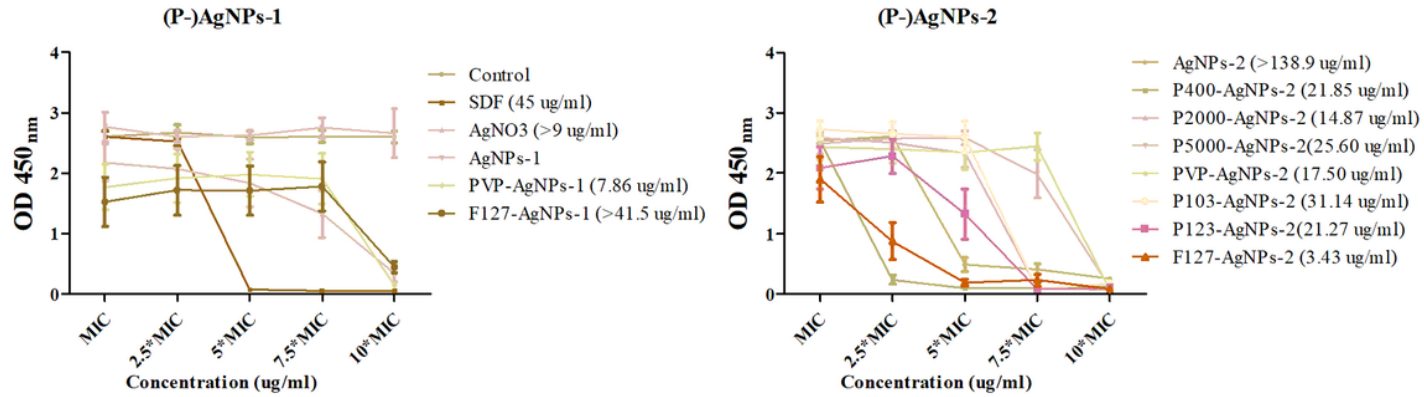

Figure 5

The dose-dependent antibiofilm effect of AgNPs-1/2 and P-AgNPs-1/2 on *P. gingivilis* biofilm (CCK8 kit). In parentheses is the minimize antibiofilm concentration of AgNPs-1/2 and P-AgNPs-1/2.

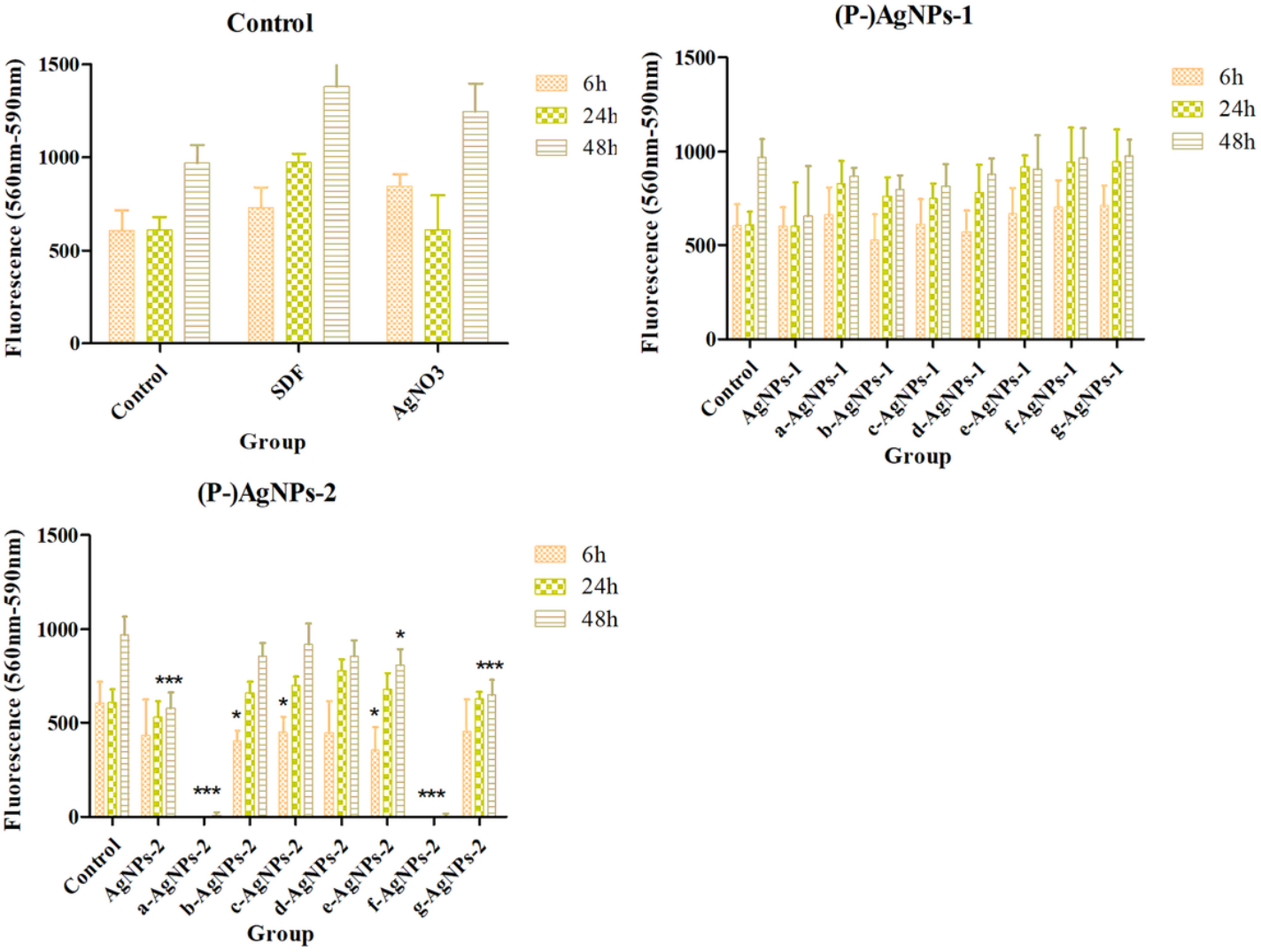

Figure 6

Cytotoxicity of AgNPs-1/2 and P-AgNPs-1/2 on Human gingival fibroblasts at 6 h, 24 h, and 48 h. ‘*’ P<0.05, ‘**’ 0.05<P<0.005, ‘***’ P<0.001.

Supplementary Files

This is a list of supplementary files associated with this preprint. Click to download.

- Scheme.tif